Digital Surface Models and Building Extraction: a Comparison of IFSAR and LIDAR Data

P. Gamba, *Member, IEEE* and B. Houshmand, *Member, IEEE*

P. Gamba is with Dipartimento di Elettronica, Università di Pavia, Via Ferrata, 1, I-27100 Pavia, Italy. B. Houshmand is with Jet Propulsion Laboratory, 4800 Oak Grove Drive, Pasadena, CA. The research described in this paper was carried out by the Jet Propulsion Laboratory, California Institute of Technology, under a contract with the National Aeronautics and Space Administration.

Abstract

In this paper the task to extract significant built structure in Digital Surface Models is analyzed. The original data are obtained by means of Interferometric SAR or LIDAR techniques, and have different resolution and noise characteristics.

This work aims to make a comparison of what (and how precisely) it is possible to detect and extract starting from these models, taking into account their differences, but applying to them the same planar approximation approach. To this aim, data over Los Angeles and Denver is considered and evaluated.

The results shows that LIDAR data provide a better shape characterization of each building, not only because of their higher resolution. Indeed, less accurate results obtained starting from radar data are mainly due to shadowing/layover effects, that can be only partially corrected by means of the segmentation procedures. However, better results than those already presented in literature could be achieved by using the IFSAR data correlation map.

I. Introduction

The three-dimensional structure of a urban environment is extremely complex, and crowded with objects of different nature and height. Commercial buildings, residential areas, green areas with trees and fences, roads and railroads passing one over the other: each of these groups represents objects with different material, spatial and spectral characteristics, variously interacting one with the others. Anyway, the precise knowledge of this structure is useful not only to identify all these elements of the urban landscape, but also to highlight their interactions with the natural landscape. Moreover, towns and cities are characterized by a fast changing rate, and all the activities that rely on a accurate characteristic detection (from urban planning to real estate monitoring, from hazard prevention to insurance) need a method to update urban data efficiently and reliably [1].

This is the reason why there is a growing interest in developing sensors and tools aimed to the detection mainly of all the man-made 3D landscape features, with reasonable costs and reduced working time. And this is also the reason why 3D measurements of urban environments are moving from accurate (but long, expensive and largely time-consuming) photogrammetric techniques to other systems, like interferometric radar (IFSAR) and laser altimeters (LIDAR). As a consequence, even image analysis techniques for 3D structure detection, noise correction, and automatic urban landscape reconstruction have been

introduced [2], [3].

Analysis of the IFSAR terrain elevation data in urban areas are usually difficult due to the insufficient spatial resolution, multiple scattering due to the building geometries, and layover effects, in addition to the intrinsic IFSAR system level noise. Therefore, there is still a strong need to evaluate which kind of information is available from these data and to what extent it is possible to extract them. The resolution problem is being increasingly resolved by the new generation of radar sensors operational in the near future: the goal of these systems is to provide a 1-meter level spatial resolution, which therefore can resolve many of the objects present in an urban environment [4]. As for the second problem (multi-scattering, layover, and noise), we found very interesting to apply to the original remote sensing images some suitable machine vision approaches [5].

LIDAR data are increasingly used for urban landscape definition [6], [7], due to their accuracy both in height and range measurements. For instance, several applications (from tornado damage assessment to power line detection) were listed in [8], as well as a railroad GIS design [9]. LIDAR may be carried by light airplanes or helicopters, and is cheap to buy and operate. It should be noted however that some issues in data accuracy are still open, especially with respect to data analysis and filtering, as noted in [11]. More work is needed, among the other problems, for building extraction, both to build 3D city models, and to find Digital Elevation Models (DEMs) of the ground, where man-made features must be discarded [10].

The aim of this work is to use a simple yet powerful technique that we developed for the analysis of IFSAR data to make a comparison of what we can extract (in a automatic way) from data recorded in different places (the Santa Monica area in Los Angeles and the State Capitol area in Denver) by means of an high precision C-band SAR and a commercially available laser altimeter.

The paper is organized as follows: Section II presents a brief overview of the use of digital surface models for building extraction, Section III summarizes the building extraction algorithm that we used, Section IV shows the experimental results, while in Section V these results are discussed. Finally, Section VI concludes the paper.

II. Non-photogrammetric DSM and building extraction: an overview

There is a large literature referring to photogrammetric extraction techniques for Digital Surface Models (DSM) in towns (see for instance [12]), but only a few articles about the same topic and LIDAR. A comprehensive comparison of laser altimetry and digital photogrammetry, with a section dedicated to DSM/DTM (Digital Terrain Model) generation can be found in [13]. Moreover, almost nothing has been published about the use of IFSAR data to compute precise DSMs of urban areas. Therefore, even if this overview is far from being exhaustive of the topic, its idea is to explore this area to understand where and how more research is needed.

The high precision LIDAR data which is now available from commercial airborne or helicopter-mounted laser altimeters allow the use of building extraction algorithms which were originally developed for photogrammetric data. The usual approach starts from applying mathematical morphology filters to the original LIDAR data to extract the terrain surface (and deny buildings and vegetation), called Digital Elevation Model (DEM). After subtracting the DEM from the original data, the objects higher than ground level are retrieved by means of a thresholding procedure (possibly hierarchical, like in [14]). Vegetation and man-made features are discriminated using a suitable spatial filter, based for instance on reflectance measurements [15] or differential geometry concepts [16]. In the first case, the information carried by the laser beam is used not only to compute the distance between the illuminated surface and the source, but also to characterize its physical properties (material, roughness, ...). This additional information is used to discriminate between reasonably flat man-made structures and highly corrugated, more absorbing trees and canopies. Very similar concepts apply using differential geometry properties to recognize vegetation: the extreme variety of the top surface of green areas reflects into very high spatial variance and deep step edges in these zones. Therefore, an investigation on these quantities allows to easily recognize buildings that do not possess such characteristics. The work may be done either when resampling the sparse LIDAR measurements into the final image grid (so called *intra-cell variance*) or by considering the variance of the normal to the surface direction in neighboring cells. Both methods provide sufficiently accurate discrimination between man-made features and vegetation, even if the reflectance

classification achieves better results.

The detected buildings are then examined and usually the best fitting polyhedral model is chosen by extracting the roof planes and their mutual spatial relationships. To this aim, in [17] the height and size of segments are used to refine parametric and prismatic models, while in [20] the planar surfaces obtained by the previous steps are jointly evaluated, and their parameters compared to find the best way to represent the structure. However, none of these methods is sufficient to extract valid Computer Aided Design (CAD) city models, and the best results are still based on semi-automatic approaches where the operator corrects the final results of the previous algorithms. More sophisticated analyses try to recognize the roof model from a set of sparse (but significant) 3D points representing the top of a building. This may be done by applying photogrammetric analysis methods like [18], [19] to the set of points belonging to the boundary (somehow ordered) together with some interior points randomly added.

Open problems with respect to LIDAR data, together with better model extraction procedures, are to find the limit of what it is possible to extract, in terms of the target dimensions and material characteristics, and which are the most suitable algorithms to achieve these results.

Radar-derived 3D images are far more difficult to analyze, not only because radar systems are not able to extract information with the same spatial and vertical resolutions, but also because they are affected by different problems, due to the stronger interaction of the electromagnetic fields with urban materials in the microwave range than at the optical wavelengths. In particular, the line-of-sight masking and the multiple reflections from the walls produce phase artifacts, giving raise to the so called *shadowing* and *layover* effects. So, the typical response of a large building as computed from the IFSAR data comprises a large zone in the direction of the sensor, realizing a sort of "reverse tail", that cancels the sharp edge characterizing the original surface, and also a similarly large area from the other side of the object, where no measurements were possible and so no data is assigned.

Therefore, the largest problem in the interpretation of these data is how to reconstruct the original structure of the surfaces illuminated by the radar. In [21], for instance, algorithms based on heuristics are applied to better retrieve the building edge, and therefore its

correct footprint. In [22], instead, a more global approach is introduced, trying to segment the data while denoising them with a machine-vision model-based approach. Still, even if the DSM resolution is coarser than in the LIDAR final grid, useful information could be extracted, and further work is necessary to refine the height and footprint analysis methods, as well as to go towards an automatic 3D model definition for each object.

III. The building extraction method

In this work we focus on the task to extract information on urban structures from medium/high resolution Digital Surface Models: specifically, we want to automate the detection of the height and shape of the buildings in a given area. To this aim, we apply to the original data a segmentation algorithm to exploit both the spatial and vertical resolutions, while maintaining at the same time a high robustness to noise. In particular, the criteria applied to segment the raw data are geometric ones, involving the principle of plane-fitting (i.e. to find the plane which better approximates a given surface): in our situation this approach corresponds to look for the building roofs and walls. Neglecting the simple iterative region growing approach, we may start from a different version of the algorithm outlined in [22], which in turn is a modified version of [23].

The algorithm starts from primitives of segmentation that are the lines of the image, in order to save cpu time as much as possible, and it works by means of five processing steps.

1. First, we group the pixels of each line into segments according to the following geometric criterion: a line is initially broken if an edge is detected (by comparison with a step threshold) and resulting segments are further subdivided if their middle point is too far from the actual data. This procedure is iterated until it is possible to find a breakpoint or down to the smallest segment length allowed. We will see in the discussion that it is a good practice to set this length as small as possible with respect to the physical characteristics of the buildings to be extracted and the resolution of the image.
2. The second step consists in finding the *seeds* for the planar surfaces that we want to use to characterize the original image. Differently from the previous version of the algorithm presented in [22], each seed is found by looking only for two adjacent segments belonging to two successive scan lines and with the most similar direction

and z-axis intercept. So, similarity search is based on the following measure

$$s_{ij} = \frac{1}{2}\left(\frac{m_i m_j + 1}{\sqrt{(m_i^2+1)(m_j^2+1)}} + \frac{n_i n_j + 1}{\sqrt{(n_i^2+1)(n_j^2+1)}}\right) \quad (1)$$

where $z = m_i x + n_i$ is the generic segment equation. One of the reasons for this simple seed choice is just its simplicity; however, the main reason is that, dealing with complex buildings, the number of three-segment seeds that we may find is definitely lower than the one of two-segment seeds. Therefore, the successive region growing procedure may suffer from this problem and aggregate only a small number of other segments to the original seeds.

3. Indeed, the second step of the building segmentation procedure starts when all the segments adjacent to each seed are examined: if a segment is close enough (again with respect to both its slope and intercept) to the plane which better approximates the seeds, it is added to the region. This process is applied to all the seeds and iterated (considering the new aggregated regions), until no more expansion is possible, and (hopefully) the image is divided in planes.
4. Since the choice of the threshold used to aggregate the segments to the seeds has a large impact on the final result (tighter values leave a large number of unaggregated segments, for instance) a further merging step takes into account separately the pixels left, trying to merge them with the nearest plane. Even in this case the process is iterated after recomputing the plane parameters until no further refinement is possible.
5. Finally, the recovered planes may be grouped if they are adjacent and their characteristics are similar, i. e. again

$$s = \frac{1}{3}\left(\frac{aa' + 1}{\sqrt{(a^2+1)(a'^2+1)}} + \frac{bb' + 1}{\sqrt{(b^2+1)(b'^2+1)}} + \frac{cc' + 1}{\sqrt{(c^2+1)(c'^2+1)}}\right) \quad (2)$$

is close to one, $\{a, b, c\}$ being the three parameters identifying a plane.

As a last comment, we should note that not all the pixels must necessarily belong to a plane, and therefore at the end of the procedure all the points affected by large noise, or regions where no actually planar surface is observable are left ungrouped.

IV. Experimental results

The previously presented algorithm was applied to two different test sets. The first is an interferometric SAR derived surface model with medium precision (5 m posting). The data were obtained with the AIRSAR system, operated by NASA/JPL and mounted on a DC8 plane. The system works at C-band (5.6689 cm wavelength) with a 40 MHz pulse bandwidth, and has a nominal height accuracy in the order of $\pm$ 2.5 m. After the interferometric processing [24], [25], the ground range resolution for the mid-swath area is about 10 meters, and the elevation data are provided at 5 meter postings, geocoded and rectified.

The LIDAR DSM was obtained by means of a commercial laser altimeter incorporated into the sensor instrumentation package called DATIS (Digital Airborne Topographical Imaging System) and operated by EagleScan, Inc., in Boulder, CO. The system, in its high resolution operation mode, provides a mean sample density of 9 to 15 feet (nearly 3 to 5 meters), a slightly coarser resolution than other commercial packages [11]. Vertical accuracy meets the requirements of 15 cm root mean square error. The original data are not placed on a grid, so that the re-sampling procedure was achieved by taking the mean of all the samples inside a given grid element. The final DSM may have positions without measurements, and their value is provided by considering the mean of neighboring cells. Three choices for the final sample posting were made:

- 10 meter, for comparison with the resolution of the AIRSAR DSM;[1]
- 5 meter, for comparison with the 5 meter posting DSM (even though the resolution is 10 meters);
- 3 m. for the LIDAR resolution.

An interesting problem to be evaluated is whether it is possible to use the same building extraction procedure for both SAR and LIDAR datasets, and how its parameters must be changed accordingly. Moreover, we would like to understand from these experiments what it is possible to extract from these two different sets of measurements in terms of object

[1]Currently, 80 MHz, X-band data is commercially available at 2.5, 5, and 10 meter postings from Intermap, Inc. We intend to use the 80 Mhz data for the Denver area (when they will be available) to examine and compare the performance of our building extraction algorithm.

characteristics (essentially, building footprint, height and shape).

A. Building extraction from IFSAR data

The interferometric SAR image used in this research covers a portion of the metropolitan area of Los Angeles (exactly, a part of Wilshire Boulevard, S. Monica). The images we show here come from a larger data series recorded on August 5, 1994, from the height of 11.000 meters. The flight path was from 33.97 N latitude, -118.47 longitude to 33.97 N latitude, -118.41 longitude. Ground truth was provided by using available 3D CAD models, or by a field recognition of the buildings, and the measurement, as accurate as possible, of their footprints and heights.

Fig. 1 presents the original data, while fig. 2 shows the same data after applying the algorithm outlined in section III, with the most relevant structures individuated and extracted. The importance of this result is twofold. First, each of the buildings is reconstructed and the noise or shadowing/layover effect has been partially discarded. Second, each extracted structure is completely isolated from the others, providing an "intelligent" segmentation of the original DSM.

In [5] and [22] we applied a similar procedure to the same data set, finding that the building height accuracy is almost within the precision of the AIRSAR sensor (± 2.5 m). So, we may say that the inaccuracies introduced by the grouping algorithm are negligible. However, in that paper it was found that the algorithm led to (heavy) underestimates of the building footprints. The underestimate was due principally to the fact that we considered only the flat top of each building as a representative of its footprint. In this improved version of the algorithm no flat top is provided, because we try to reconstruct as faithfully as possible the shape of the buildings. For sake of comparison, we assumed as footprint of each extracted object the area that it occupies at the mean roof level (the mean level of the roofs of the small residential buildings all around it). Correspondingly, we considered as the height of a building the mean value of the highest plane inside its footprint (we used the mean and not the maximum value to discard possible outliers).

Considering these definitions, the current version of the building extraction algorithm provides results comparable to those in [5] and [22] with respect to the heights extracted, while for the footprints it gives more reliable values, as it can be seen in Table I, that

compares the percentage area errors of the target buildings in the area. Negative values correspond to underestimates (mainly due to shadowing effect), positive ones to overestimates (for buildings with large layover effects). A look at the table reveals that the new method usually overestimates the building section, but the mean square value of the area error has decreased, if we consider the same test set. For the 5 buildings considered in both papers this value is now 18% instead of 20%.

Finally, in the same table further results are presented, obtained when we used jointly the 3D IFSAR data and the SAR measurements correlation map, i. e. an image representing in each point the correlation among the SAR measurements in that point and a region around it [24]. The idea is that false heights due to shadowing/layover effects should have lower correlation than actual measurements. Indeed, low correlation corresponds to a larger interferometric phase noise, which in turn reduces the accuracy of the IFSAR DSM. Therefore, by discarding low correlation pixels we may have a more precise 3D image of any area. We found that, by considering only 3D data extracted from measurements with correlation value higher than 0.5, we obtained better results (those in the last column of Table I), where the mean square area error is now even less. However, the area where no data is available has been dramatically increased and Barrington Plaza Apt. I now splits into two distinct objects.

B. Building extraction from LIDAR data

The LIDAR data considered in this subsection refer to downtown Denver, and precisely to the area around the Colorado Capitol and covering the park in front of it and some of the buildings around. The original data at 5 and 10 m resolution respectively are depicted in fig. 4 and 5, while an aerial image of the same area at higher resolution (nearly 1 m) is shown in fig. 3. Many buildings with different shapes can be easily recognized from the DSM, even at the coarse resolution.

However, a closer look reveals that the re-mapped image grid does not provide the same vertical resolution granted for each measurement, and therefore, even if extremely detailed, the DSM is also noisy. This is evident, for instance, by looking at fig. 6, where the Colorado State Capitol at three different resolution (10, 5 and 3 m) is shown. It is clear that the task to extract a meaningful structure model is more complex than at a first glance.

Fig. 4 and 5 provide the best results that we were able to obtain with the building extraction algorithm on the 5 and 10 m data sets. In the resulting DSMs only the points that were aggregated into planes are drawn, to show that the analysis provides a joint de-noising and segmentation of the original data. Many of the missing points are however aggregated into segments, that are too different in orientation to be joined to neighboring planes. This is mainly an effect of the imprecision of the original data, as it can be seen in fig. 7, where three successive lines of the 5 m Capitol data (center image in fig.6) are depicted. It is clear that the building profile change very much from one line to the other, and it is difficult to find reliable relationships among the linear approximations.

It should be noted that for this data set no measurement point was discarded at the input of the segmentation procedure, because LIDAR data are not affected by shadowing and/or layover effects. Instead, much more attention had to be paid to the choice of the line segmentation parameters, to make the detection algorithm robust with respect to the local noise ripple . Table II summarizes the best results achieved for the Colorado State Capitol by giving the area percentage error at the three different analyzed resolutions using very similar sets of input parameters, together with the output 3D profile (to be compared with fig. 6). Note that the choice of suitable input values for the parameters will be discussed in detailed in the next session.

V. Discussion of the results

The results of the preceding section were obtained by a suitable choice of the thresholds and parameters involved in the segmentation procedure. Moreover, more information than the 3D reconstructed urban profile was used, when available from the original sensor. However, these choices must be discussed, and the utility of these additional data is also to be considered.

In particular, as already observed, SAR data over Los Angeles, suffer from overlay/shadowing effects. They prevent the algorithm from finding the actual 3D shapes if we do not introduce some *a priori* information about the reliability of the measurements and where they can (or must) be discarded. To this aim, the correlation map was added to the original DSM, to provide a manner to quantify this reliability. The threshold on the correlation value was chosen exactly in the middle of its range of values; we should add that a slight

change of this threshold toward raising values produces mixed results. Indeed, on one hand many other uncertain pixels are discarded; on the other hand, also meaningful information begins to be lost. Therefore, from these results we observed that the intuitive choice of 0.5 can be considered also the best one. The parameters for the building extraction procedure were chosen according to [5], i. e. overpartitioning the scan lines and allowing the segment length to be as small as two pixels (10 m).

Since information similar to the correlation map were not available for the LIDAR data, we focused only on the choice of the parameter values to segment the original image in the best possible way. We maintain fixed to the minimum reasonable value the distance between the middle point of each segment and the actual corresponding 3D point (say, 1 m) and the segment length (2 pixels). We analyze here how to choose the step threshold and the similarity required for segment aggregation (see section III). The results were evaluated by means of five parameters: percentage error on area with respect to the original data, mean height error and corresponding standard deviation, mean height error and corresponding standard deviation after discarding the points that are still isolated at the end of the procedure.

Fig. 8(a) depicts the behavior of these quality measures with respect to the step threshold value with similarity value fixed to 0.6: it is clear that higher step values produce worse results, but the $[2 \div 5]$ range is almost equally valuable, and this is strictly connected to the local fluctuation of 3D points around their actual value (see for instance fig. 7). In fig. 8(b), instead, taking the step threshold fixed to 3 m, the similarity requirements were changed. The first, truly interesting, result is that lower values give better outcomes, up to no area error. This is due to the strong requirements in segment definition (i. e. the 1 m segment division threshold and the 2 pixel minimum length) so that segments are only *nominally* poorly similar. In other words, even if you join two adjacent segments 2 pixels long in a single plane, it is almost immaterial which is their original slope and intersect: the plane is so small that no large error may result!

A further advantage of this choice is that the final structure is obtained by means of a large number of segment-plane associations and a small number of final point aggregations (and so, shorter cpu-times). The disadvantage is that there are many planes representing

the same structure. and if we want to merge them we may use the same threshold, allowing possibly large final errors, or a tighter one, with the danger not to aggregate elements at all (since they are too different planes).

As a final comment to the algorithm (in both analysis situations), we should note that the idea to take as primitives the image line segments introduce a privileged direction in the segmentation procedure. This choice has no influence on the results when the surfaces to be retrieved are large with respect to the starting segment primitives, as in the original application [23]. In our IFSAR and LIDAR images, instead, building dimensions can only be a few pixels wide, and as a result this direction must be carefully chosen. Therefore, if the environment to be analyzed (like in almost any urban situation) contains randomly oriented objects, the detection and reconstruction accuracy may be a decreasing function of the angle between the segmentation and the building direction.

VI. Conclusions

This work shows that it is possible to develop a common procedure for 3D building detection and extraction from DSMs, even if originating from different sources. We applied our algorithm to IFSAR and LIDAR derived surface data to examine its performances, and evaluate the data characteristics. The same procedure was also used to understand which are the potentiality and the drawbacks of the two different data sets, namely IFSAR elevation maps and LIDAR range measurements. We specified a detailed procedure to choose the parameters of the building extraction method starting from the knowledge of the horizontal and vertical resolutions of the original DSMs.

Our algorithm was successful in automatic detection and extraction of relatively large, isolated structures for both data sets. This is consistent with the available data postings (3 meter for LIDAR, and 5 meter for IFSAR). The mean footprint of the well detected buildings is around 1800 m^2, but we had very good results even for 11645 Wilshire Boulevard (see Table I), whose footprint is less than 900 m^2.

LIDAR data was characterized with higher vertical precision. This high precision is balanced with the extended time which is required for high resolution data acquisition. A reduction in acquisition time is possible by using a scanning LIDAR system, which in turn will suffer from shadowing effects.

IFSAR data acquisition is rapid, but for urban areas it suffers from layover (for the radar illuminated side of the building) and shadowing (this corresponds to multiple reflections, where a height value is reported in the region where no data can be available due to blockage of the radar signal by the structure) due to the presence of large structures. Also, the multiple scattering effects produces artifacts which should be taken into account. We used the interferometric correlation coefficient to eliminate the height values which can reduce the performance of our extraction algorithm. We found that by using the correlation value of 0.5, the height values around dominant structures which can be corrupted by layover and shadowing are masked out for the purpose of automated detection and extraction. However, even with this correction, the 3D profiles and 2D footprints of the buildings suffer from under- or overestimate.

Future developments could be additional pre-processing algorithms to discard as much as possible the multiple scattering effects on the radar backscattered signal, before applying the clustering step. A possibility could be to jointly evaluate coarse LIDAR acquisitions and IFSAR elevation data. Finally, a more refined version of the detection algorithm, based on a direct plane fitting (avoiding the clustering problems highlighted above) is under development.

Moreover, the incidence angle is surely a variable to consider when dealing with IFSAR derived DSMs. Indeed, the detection procedure outlined in this paper was designed to "correct" the shadowing/layover shape errors and should be independent from the *quality* of the DSM. Practically, however, we may have different results for the same test set starting from different IFSAR measurements. So, one of the research directions we are exploring now is to characterize urban DSMs derived from near or far-range radar data.

Acknowledgments

LIDAR data were kindly provided by EagleScan, Inc., Denver, CO.

References

[1] F.M. Henderson and Z.G. Xia, "SAR applications in human settlement detection, population estimation and urban land use pattern analysis: a status report," *IEEE Trans. on Geoscience and Remote Sensing*, Vol. 35, No. 1, pp. 79-85, 1997.

[2] N. Haala and C. Brenner, "Extraction of buildings and trees in urban environments," *ISPRS J. Photogramm. Remote Sensing*, Vol. 54, No. 2-3, pp. 130-137, July 1999.

[3] H.-G. Maas and G. Vosselman, "Two algorithms for extracting building models from raw laser altimetry data," *ISPRS J. Photogramm. Remote Sensing*, Vol. 54, No. 2-3, pp. 153-163, July 1999.

[4] M. Coltelli. G. Fornaro, G. Franceschetti, R. Lanari, A. Moreira, E. Sansoti, R. Scheiber, M. Tesauro, T.I Stein, "Results of the Mt. Etna interferometric E-SAR campaign," Proc. of *IGARSS'97*, Vol. IV, pp. 1554-1556, Singapore, Aug. 1997.

[5] P. Gamba, B. Houshmand, M. Saccani, "Detection and extraction of buildings from interferometric SAR data," *IEEE Trans. on Geoscience and Remote Sensing*, to be published.

[6] L. Zhen, L. Shukai, "A new airborne remote sensing system integrating scanning altimeter with infrared scanner," Proc. of *IGARSS'97*, Vol. I, pp. 427-429, Singapore, Aug. 1997.

[7] D.L. Rabine, J.L. Buffon, C.R. Vaughn, "Development and test of a raster scanning laser altimeter for high resolution airborne measurements of topography," Proc. of *IGARSS'96*, Vol. I, pp. 423-426, Lincoln, Nebraska, May 1996.

[8] B. Gutelius, "Engineering applications of airborne scanning lasers: reports from the field," *Photogrammetric Eng. Remote Sensing*, Vol. 64, No. 4, pp. 246-253, Apr. 1998.

[9] A.J. Lembo, Jr., C. Powers, E.S. Gorin, "The use of innovative techniques in support of enterprise wide GIS development," *Photogrammetric Eng. Remote Sensing*, Vol. 64, No. 9, pp. 861-865, Sept. 1998.

[10] M.J.P.M. Lemmens, "Accurate height information from airborne laser-altimetry," Proc. of *IGARSS'97*, Vol. I, pp. 423-426, Singapore, Aug. 1997.

[11] E.J. Huising, L.M. Gomes Pereira, "Errors and accuracy estimates of laser data acquired by various laser scanning systems for topographic applications," *ISPRS J. Photogramm. Remote Sensing*, Vol. 53, No. 5, pp. 245-261, Oct. 1998.

[12] E.P. Baltsavias, S. Mason, and D. Stallmann, "Use of DTMs/DSMs and orthoimages to support building extraction," in *Automatic Extraction of Man-Made Objects from Aerial and Space Images*, A. Grun, O. Kubler and P. Agouris, Eds., 1995, pp. 199-210, Birkhauser, Basel.

[13] E.P. Baltsavias, "A comparison between photogrammetry and lase scanning," *ISPRS J. Photogramm. Remote Sensing*, Vol. 54, No. 2-3, pp. 83-94, July 1999.

[14] A. Brunn, E. Gulch, F. Lang, W. Forstner, "A hybrid concept for 3D building acquisition," *ISPRS J. Photogramm. Remote Sensing*, Vol. 53, No. 1, pp. 119-128, Feb. 1998.

[15] C. Hug, A. Wehr, "3D reconstruction and modeling of topographic objects," IAPRS, Vol. 32, Part3-4W2, Stuttgart, Sep. 17-19, 1997.

[16] C. Hug, "Extracting artificial objects from airborne laser scanner data," in: Gruen, A., Baltavias, E, Henricsson, O. (Eds.), Automatic extraction of man-made objects from aerial and space images (II), Birkhauser, Basel, pp. 203-212, 1997.

[17] U. Weidner, W. Forstner, "Towards automatic building extraction from high resolution digital elevation models," *ISPRS J. Photogramm. Remote Sensing*, Vol. 50, No. 4, pp. 38-49, Aug. 1995.

[18] A. Gruen, X. Wang, "CC-modeler: a topology generator for 3-D city models," *ISPRS J. Photogramm. Remote Sensing*, Vol. 53, No. 5, pp. 286-295, Oct. 1998.

[19] A. Gruen, "TOBAGO - a semi-automated approach for the generation of 3-D building models," *ISPRS J. Photogramm. Remote Sensing*, Vol. 53, No. 2, pp. 108-118, Apr. 1998.

[20] A. Brunn, U. Weidner, "Hierarchical Bayesian nets for building extraction using dense digital surface models," *ISPRS J. Photogramm. Remote Sensing*, Vol. 53, No. 5, pp. 296-307, Oct. 1998.

[21] G.R.Burkhart, Z. Bergen, R. Carande, W. Hensley, D. Bickel, J.R. Fellerhoff, "Elevation correction and building extraction from Interferometric SAR imagery," Proc. of *IGARSS'96*, Vol. I, pp. 659-661, Lincoln, Nebraska, July 1996.

[22] P. Gamba, B. Houshmand, "Three-dimensional urban characterization by means of IFSAR measurements," to be published in the Proc. of *IGARSS'99*, Hamburg, Germany, June, 28 - July, 2, 1999.

[23] X. Jiang and H. Bunke, "Fast segmentation of range images into planar regions by scan line grouping," *Machine Vision and Applications*, No. 7, pp. 115-122, 1994.

[24] H.A. Zebker, S.N. Madsen, J.M. Martin, K.B. Wheeler, T. Miller, Y. Lou, G. Alberti, S. Vetrella, A. Cucci, "The TOPSAR interferometric radar orographic mapping instrument," *IEEE Trans. on Geoscience and Remote Sensing*, Vol. 30, No. 5, pp. 933-940, 1992.

[25] S.N. Madsen, J.M. Martin, H.A. Zebker, "Analysis and evaluation of the NASA/JPL TOPSAR across-track interferometric SAR system," *IEEE Trans. on Geoscience and Remote Sensing*, Vol. 33, No. 2, pp. 383-391, 1995.

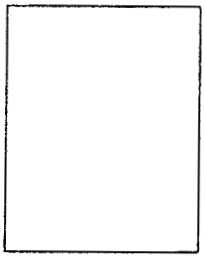

Paolo Gamba was born in Cremona, Italy, on April 5, 1965. He received the Laurea degree in Electronic Engineering "cum laude" from the University of Pavia, Italy, in 1989. He received also from the same University the Ph.D. in Electromagnetics in 1993.

From 1992 to 1994 he was a R&D engineer in the Microwave Laboratory of Siemens Telecomunicazioni, Cassina de' Pecchi, Milano, Italy. In 1994 he joined the Department of Electronics of the University of Pavia where now is Assistant Professor and teaches Radiocommunications Systems.

His current research interests include the application of machine vision approaches to GPR images, aerial and satellite SAR data analysis over urban environments, metereological radar and satellite data processing.

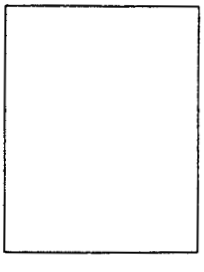

Bijàn Houshmand is with the Radar Science and Engineering, Jet Propulsion Laboratory, Pasadena, California, and an adjunct faculty in the Electrical Engineering Department at the University of California at Los Angles. His research activities include electromagnetic modeling for remote sensing applications, sensor fusion, image classification, and microwave system analysis and design. He is a Principal Investigator for Interferometric and Polarimetric phenomenology for Urban Analysis, and Assessment of Urban Areas with SRTM. Dr. Houshmand is a member of URSI commission B.

Figure Caption

- Fig. 1: The Digital Surface Model (DSM) of a part of Wilshire Boulevard, Santa Monica derived from AIRSAR interferometric measurements.

- Fig. 2: Classification results for the area in fig. 1 by means of the building extraction algorithm outlined in the text: note the regularization of the profile of the foreground buildings.

- Fig. 3: An orthophoto of the area of downtown Denver near Colorado State Capitol.

- Fig. 4: The building profiles reconstructed by the refined planar approximation proposed in this paper (a) or by the method in [22] (b) compared with the original LIDAR DSM of downtown Denver at 5 m resolution (c).

- Fig. 5: The original LIDAR DSM of downtown Denver at 10 m resolution (a) and the building profiles reconstructed by the refined planar approximation (b).

- Fig. 6: The resampled LIDAR DSM of the Colorado State Capitol building at 10 m (a), 5 m (b) and 3 m (c) resolution.

- Fig. 7: Three height profiles from adjacent lines of the 5 m Capitol data.

- Fig. 8: Area and height errors for the reconstructed structure of the Capitol State building starting from the LIDAR data at 5 m resolution for different choices of the input parameters of the segmentation procedure. y-axis units are percentages for the area error (red bar), meters for all other quantities; x-axis label format (see text for the definitions) is *min. step value/max. middle point distance/min. segment length (min. similarity).*

- Table I: Percentage area error in determining the building footprints starting from the Wilshire Boulevard IFSAR DSM.

- Table II: Colorado State Capitol 3D shape as reconstructed from LIDAR data at 3, 5 and 10 m resolution.

TABLE I

PERCENTAGE AREA ERROR IN DETERMINING THE BUILDING FOOTPRINTS STARTING FROM THE WILSHIRE BOULEVARD IFSAR DSM (N. C. = NOT CONSIDERED).

building	*ground truth area (m^2)*	*in [22]*	*this paper*	*with correlation map*
Coastal Federal Bank	1500	-20%	+85%	+77%
World Savings	2800	-25%	+6%	+9%
11755 Wilshire Boulevard	2475	-37%	+24%	0%
Barrington Plaza Apt. I	2400	-88%	-8%	-58%
11645 Wilshire Boulevard	875	-9%	+11%	+14%
Barrington Plaza Apt. II	675	n. c.	+81%	+66%
Barrington Plaza Apt. III	675	n. c.	+74%	+74%
West Wilshire Center	1500	n. c.	+1%	-13%

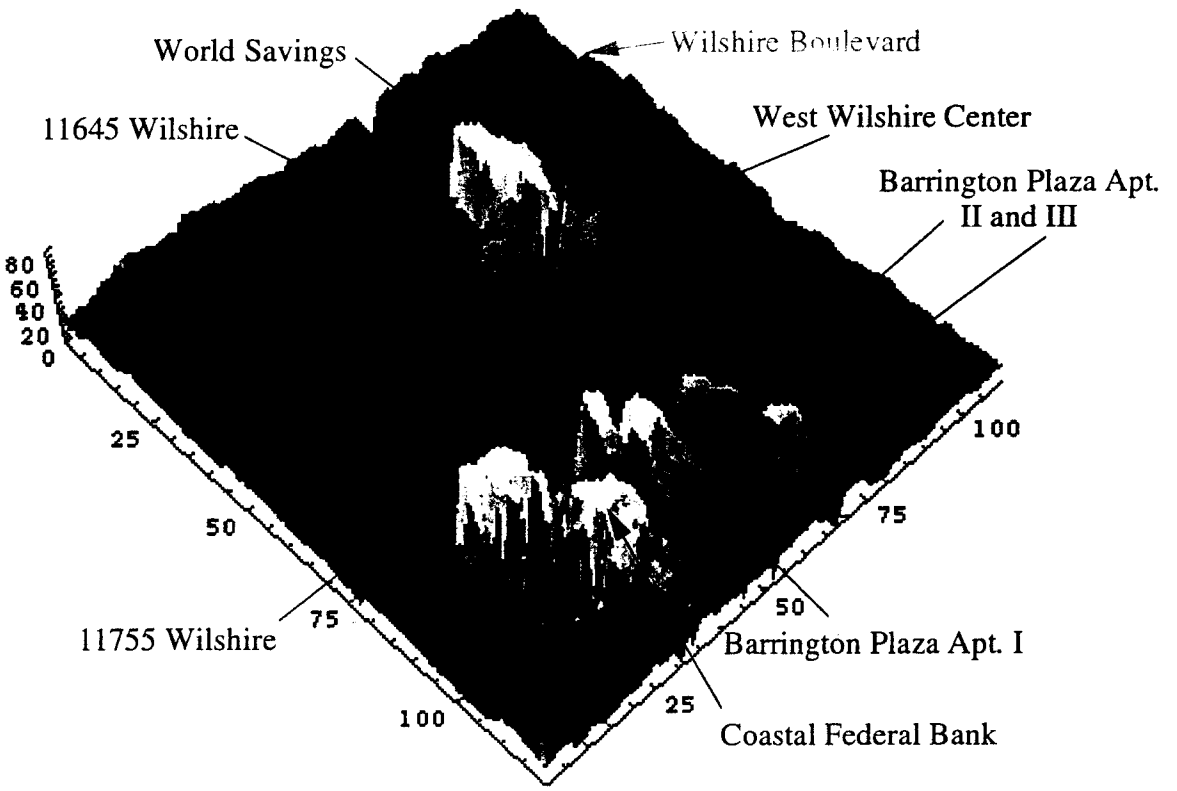
World Savings
Wilshire Boulevard
11645 Wilshire
West Wilshire Center
Barrington Plaza Apt.
II and III
80
60
40
20
0
25
50
75
100
11755 Wilshire
Barrington Plaza Apt. I
Coastal Federal Bank

fig. 1

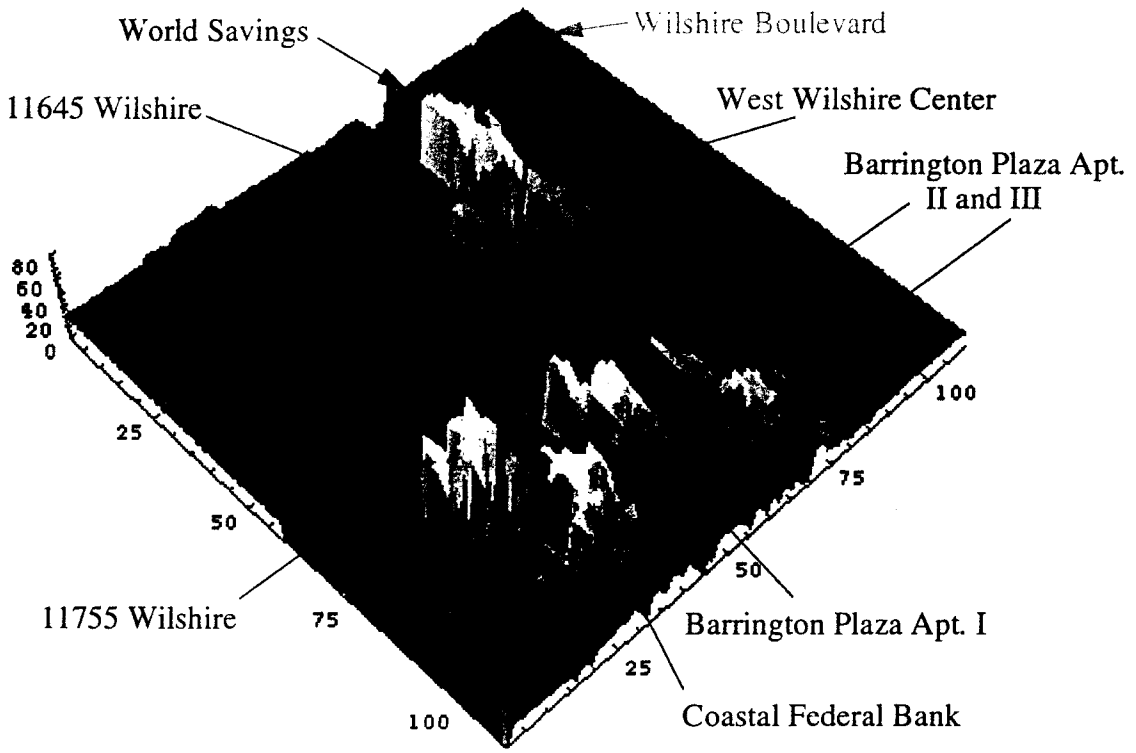
World Savings
Wilshire Boulevard
11645 Wilshire
West Wilshire Center
Barrington Plaza Apt.
II and III
80
60
40
20
0
25
50
75
100
11755 Wilshire
75
50
Barrington Plaza Apt. I
25
100
Coastal Federal Bank

fig. 2

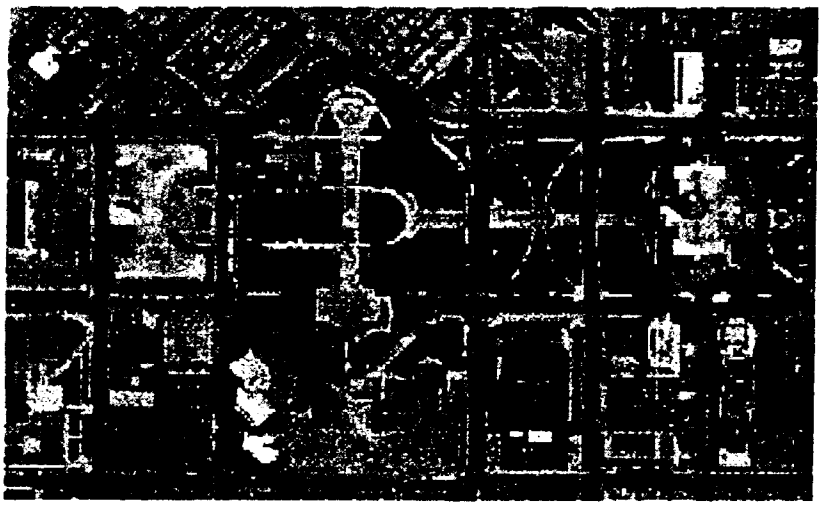

fig. 3

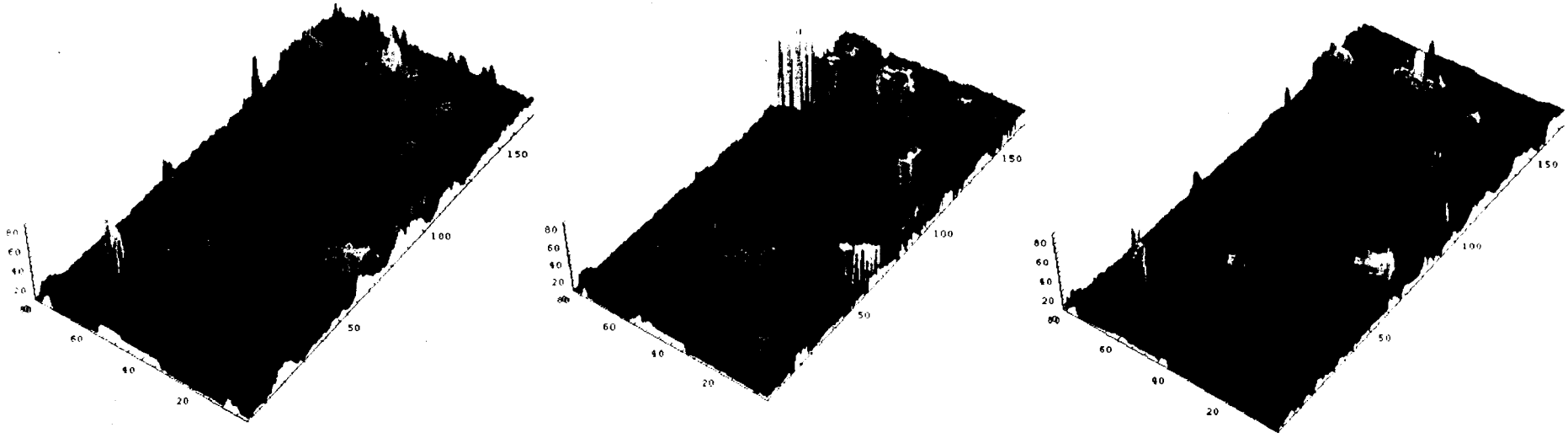
80
60
40
20
60
40
20
50
100
150
80
60
40
20
60
40
20
50
100
150
80
60
40
20
60
40
20
50
100
150

(a) (b) (c)

fig. 4

(a) (b)

fig. 5

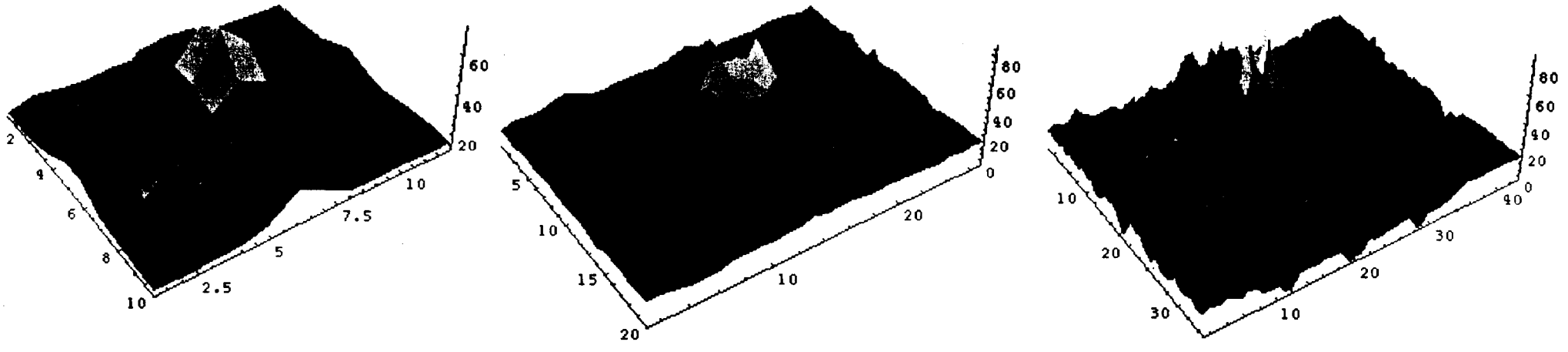
2
4
6
8
10
2.5
5
7.5
10
60
40
20
5
10
15
20
10
20
0
20
40
60
80
10
20
30
10
20
30
40
0
20
40
60
80

(a) (b) (c)

fig. 6

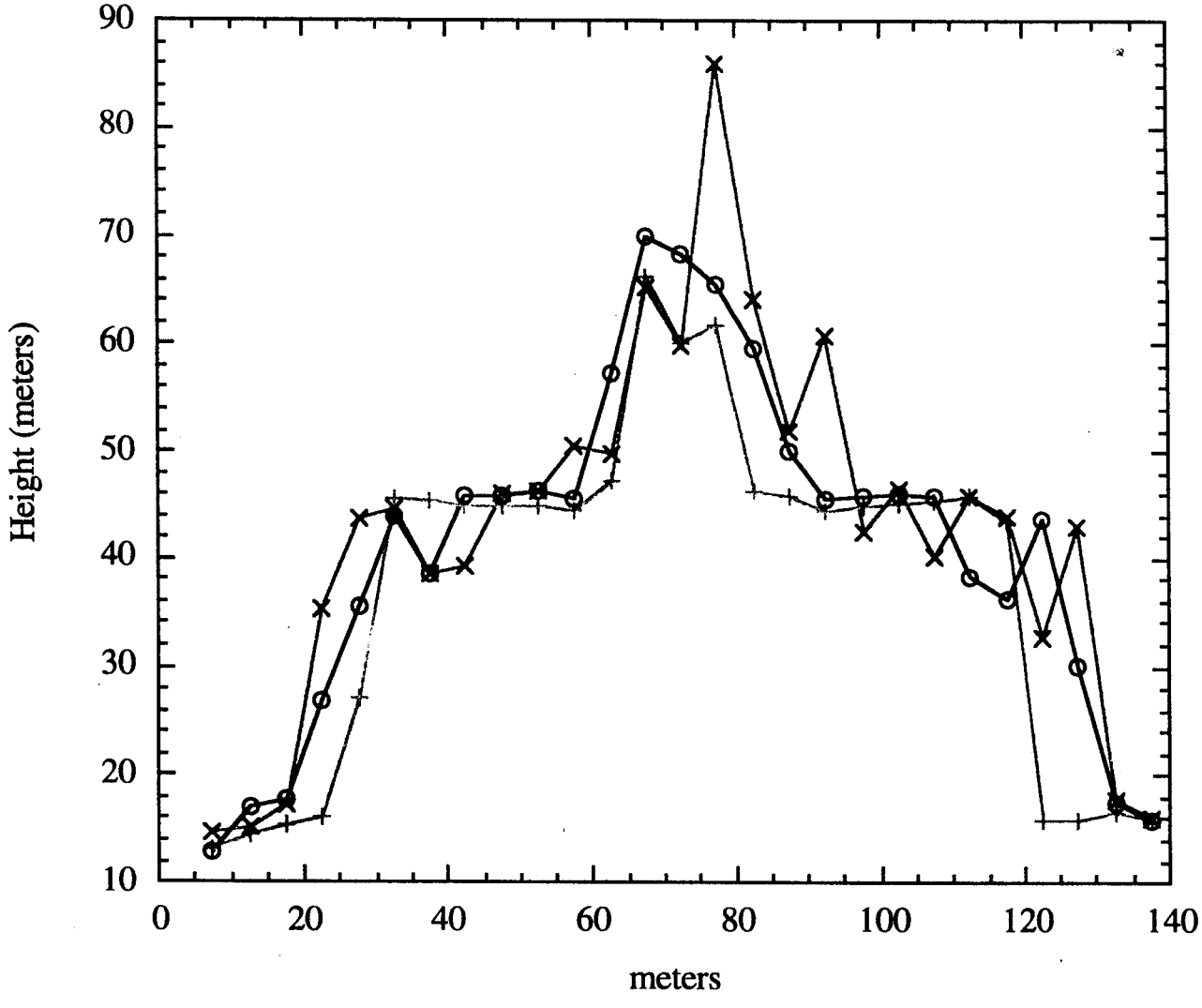
Height (meters)
90
80
70
60
50
40
30
20
10
0
20
40
60
80
100
120
140
meters

fig. 7

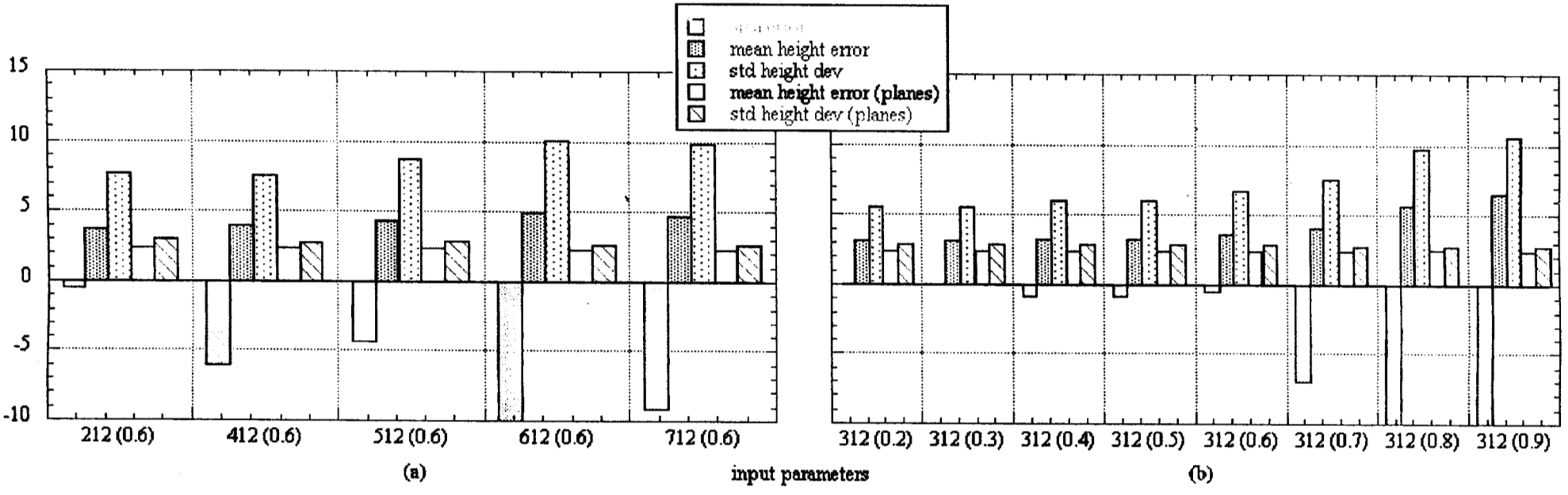
mean height error
std height dev
mean height error (planes)
std height dev (planes)
15
10
5
0
-5
-10
212 (0.6)
412 (0.6)
512 (0.6)
612 (0.6)
712 (0.6)
312 (0.2)
312 (0.3)
312 (0.4)
312 (0.5)
312 (0.6)
312 (0.7)
312 (0.8)
312 (0.9)
(a)
input parameters
(b)

fig. 8